TWMS J. App. and Eng. Math. V.16, N.2, 2026, pp. 249-265

FRACTIONAL-ORDER MODELING OF ZIKA VIRUS TRANSMISSION: ANALYSIS AND NUMERICAL SIMULATIONS

K. SHAH[1,*], J. PARMAR[1], J. PATEL[2], H. C. PATEL[3], §

Abstract. This study presents a novel mathematical framework for modeling Zika virus transmission dynamics within human populations and between humans and mosquitoes, utilizing a fractional-order Caputo derivative. The study establishes the system's feasibility region, determines equilibrium points, and analyzes their stability. The existence and uniqueness of the solution are proven using fixed-point theory, and solutions are approximated via the fractional natural decomposition method. A key novelty of this study lies in the comparative analysis of fractional-order and integer-order models, highlighting how fractional derivatives provide greater modeling flexibility and better capture memory effects in disease progression. The numerical simulations demonstrate the significant influence of fractional derivatives on system behavior, illustrating differences in the rate of infection spread and disease persistence compared to integer-order models. This fractional calculus approach offers valuable insights into the complex dynamics of Zika virus transmission. Importantly, this study explores how fractional-order modeling can enhance existing control strategies against Zika virus outbreaks, providing a more refined framework for evaluating intervention measures and improving public health decision-making.

Keywords: Zika Virus, Natural Transform (NT), Reproduction Number, Caputo Fractional Derivative, Fractional Natural Decomposition Method, Adomian Polynomial.

AMS Subject Classification: 83-02, 99A00

1. Introduction

Zika virus, a flavivirus primarily transmitted by Aedes mosquitoes, was first identified in a rhesus macaque in Uganda's Zika Forest in 1947 and subsequently in Aedes africanus

[1] Center of Education, Faculty of Mathematics, Indian Institute of Teacher Education, Gandhinagar, Gujarat, India.
e-mail: shah.kunjan5@gmail.com; ORCID: https://orcid.org/0000-0003-1269-0865.
e-mail: jparmar2503@gmail.com; ORCID: https://orcid.org/0009-0000-7413-2178.
[2] Science & Humanities Department, L. D. College of Engineering, Affiliated to Gujarat Technological University, Ahmedabad-382424, Gujarat, India.
e-mail: jspatel@ldce.ac.in; ORCID: https://orcid.org/0000-0001-6979-0272.
[3] Dr. S. & S. S. Ghandhy Government Engineering College, Surat, Gujarat, India.
e-mail: dr.prof.hcpatel@gmail.com; ORCID: https://orcid.org/0000-0001-7228-7256.
[*] Corresponding author.
§ Manuscript received: November 27, 2024; accepted: February 28, 2025.

mosquitoes in 1948 [1]. Early human cases were detected in Uganda and Tanzania in 1952. From the 1960s to the 1980s, Zika spread across equatorial Africa and Asia [1], with sporadic human cases reported. The first large outbreak in humans occurred on Yap Island in 2007 [2], marking a significant shift in the virus's epidemiological pattern. Subsequent outbreaks, including those in the Americas, highlighted the virus's potential for rapid global spread and its association with severe complications, particularly in pregnant women [3]. As of February 2022, the World Health Organization reported Zika virus transmission in 89 countries and territories, emphasizing its global health significance. The primary mode of Zika virus transmission is through the bite of an infected Aedes species mosquito, primarily Aedes aegypti and Aedes albopictus [3]. These mosquitoes are also known to transmit dengue, chikungunya, and other viruses. While less common, Zika can also be transmitted through sexual contact, blood transfusions, and from a pregnant woman to her fetus. Standing water in containers and vases provides suitable breeding habitats for Aedes mosquitoes, the primary vectors of Zika virus [4]. Aedes aegypti, in particular, prefers artificial containers for laying eggs [5]. These mosquitoes take approximately two to twelve days to develop from egg to maturity. Zika virus infection typically presents with symptoms lasting around seven days, including fever, rash, and joint pain, resembling other arboviral infections such as dengue. Studies indicate that individuals recovering from Zika virus infection develop immunity and are unlikely to experience reinfection. Given the complex dynamics of Zika virus transmission, mathematical models have played a crucial role in understanding its spread and guiding public health interventions. Traditional integer-order models have been widely used in epidemiology; however, they often struggle to capture the memory effects and heterogeneity inherent in infectious disease dynamics. Fractional calculus provides a more flexible and accurate framework by incorporating memory-dependent processes and non-local effects, making it particularly useful for modeling vector-borne diseases such as Zika.

Fractional-order models have gained increasing attention in epidemiological studies due to their ability to describe complex biological interactions more accurately than classical integer-order models. Unlike traditional models, fractional calculus accounts for long-range dependencies in transmission dynamics, allowing for a more realistic representation of disease spread. Recent studies have successfully applied fractional-order derivatives to model infectious diseases such as dengue fever, Zika, COVID-19, and plant diseases [7–11, 20–23, 23–39]. These models provide improved predictions and offer new insights into disease control strategies. Despite recent advances, challenges remain in developing robust epidemiological models that fully capture the multi-scale nature of Zika virus transmission. Researchers continue to explore optimal intervention strategies using fractional-order models, addressing factors such as vector control, human mobility, and climate change. In this study, we employ a fractional-order mathematical model to analyze the transmission dynamics of Zika virus and evaluate potential control measures. By leveraging the advantages of fractional calculus, we aim to enhance our understanding of Zika virus spread and contribute to more effective public health interventions.

1.1. **Model Formulation.** In this mathematical model we divide the human population (N_h) in two groups such as Susceptible humans (S_h) and Infected humans (I_h). So $N_h = S_h + I_h$. Similarly we devide the Mosquitoes population (N_m) in two groups such as Susceptible mosquito (S_m) and Infected mosquito (I_m). So $N_m = S_m + I_m$.

The mathematical model for zika virus, presented in [11] is as follows :

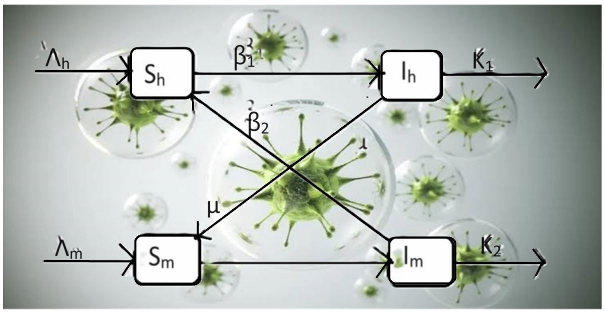

FIGURE 1. Flow Chart for Zika Virus Transmission.

$$
\begin{aligned}
\frac{dS_h}{dt} &= \Lambda_h - \beta_1 S_h I_h - \beta_2 S_h I_m - k_1 S_h \\
\frac{dI_h}{dt} &= \beta_1 S_h I_h + \beta_2 S_h I_m - k_1 I_h \\
\frac{dS_m}{dt} &= \Lambda_m - \mu S_m I_h - k_2 S_m \\
\frac{dI_m}{dt} &= \mu S_m I_h - k_2 I_m
\end{aligned}
\tag{1}
$$

List of parameter and variables used in the are :

Parameters	Description	Values
Λ_h	recruitment rate of human population	$1.2\,\text{day}^{-1}$
Λ_m	Recruitment rate of mosquito population	$0.3\,\text{day}^{-1}$
β_1	Effective contact rate of human to human	$0.125 \times 10^{-4}\,\text{day}^{-1}$
β_2	Effective contact rate of mosquito to human	$0.4 \times 10^{-4}\,\text{day}^{-1}$
μ	Effective contact rate of human to mosquito	$0.475 \times 10^{-5}\,\text{day}^{-1}$
k_1	Natural death rate of human	$0.004\,\text{day}^{-1}$
k_2	Natural death rate of mosquitoes	$0.0014\,\text{day}^{-1}$

The initial model lacks consideration for the internal memory effects inherent in the system. To enhance its accuracy, we substitute the first-order time derivative with the Caputo fractional derivative of order δ [18, 19]. With this adjustment, the transmission model for the Zika virus, applicable for $t \geq 0$ and $\delta \in (0, 1)$, is formulated as follows:

$$
\begin{aligned}
\mathcal{D}_t^\delta S_h(t) &= \Lambda_h - \beta_1 S_h I_h - \beta_2 S_h I_m - k_1 S_h \\
\mathcal{D}_t^\delta I_h(t) &= \beta_1 S_h I_h + \beta_2 S_h I_m - k_1 I_h \\
\mathcal{D}_t^\delta S_m(t) &= \Lambda_m - \mu S_m I_h - k_2 S_m \\
\mathcal{D}_t^\delta I_m(t) &= \mu S_m I_h - k_2 I_m
\end{aligned}
\tag{2}
$$

where the initial conditions are $S_h(0) = S_{0h}, I_h(0) = I_{0h}, S_m(0) = S_{0m}, I_m(0) = I_{0m}$.
We note that by a convention in epidemiology models all parameters in (2) are assumed to be positive.
Summing up the equations in (2) gives immediately the ODE system for the time evolution of the total populations of humans and mosquitos:

$$
\begin{aligned}
\mathcal{D}_t^\delta N_h(t) &= \Lambda_h - k_1 N_h(t) \\
\mathcal{D}_t^\delta N_m(t) &= \Lambda_m - k_2 N_m(t)
\end{aligned}
\tag{3}
$$

1.2. **Non-negativity and boundedness of solutions.** The positivity and boundedness of the solutions of an epidemiological system are essential properties. Therefore, it is important to prove that all subpopulations in the system (2) is non-negative and bounded for all time $t \geq 0$. The following result show how to confirm these two properties.

Theorem 1.1. *The dynamical system* (2) *exhibits boundedness for all non-negative initial conditions which are not all identically zero in the entire region given by the closed region*

$$\Omega = \left\{ (S_h, I_h, S_m, I_m) \in \mathbb{R}^4_+ \ : 0 \leq N_h \leq \frac{\Lambda_h}{k_1} \ and \ 0 \leq N_m \leq \frac{\Lambda_m}{k_2} \right\}$$

.

Proof. Assume that $\Omega = \{(S_h, I_h, S_m, I_m) \in \mathbb{R}^4_+\}$ be any solution set of the model (1) with some non-negative initial conditions such as

$$N_h(0) = S_h(0) + I_h(0) \geq 0 \tag{4}$$

corresponding to any other non-negative initial conditions on S_h, I_h. Form (3),

$$\frac{dN_h}{dt} \leq \Lambda_h - k_1 N_h(t)$$

Solving this equation leads to

$$0 \leq N_h(t) \leq \frac{\Lambda_h}{k_1} + N_{h0} e^{-k_1 t}$$

where N_{h0} is the initial value of the total population of the dynamical system. Thus, for $t \to \infty$, we have

$$0 \leq N_h(t) \leq \frac{\Lambda_h}{k_1} \tag{5}$$

Hence $N_h(t)$ is positive and bounded, and Ω is the largest set for which the solutions are positive and bounded.

Similarly, we can prove for N_m that if $N_m(0) \leq \frac{\Lambda_m}{k_2}$, then for $t > 0$, $N_m(t) \leq \frac{\Lambda_m}{k_2}$. □

1.3. **Basic Reproduction Number.** To find basic reproduction number we consider the

$$D(\Psi(t)) = F(\Psi(t)) - V(\Psi(t))$$

where F represents the Infected population and V represents the Natural death.
So,

$$F = \begin{bmatrix} \beta_1 S_h I_h + \beta_2 S_h I_m \\ \mu S_m I_h \end{bmatrix} \text{and } V = \begin{bmatrix} k_1 I_h \\ k_2 I_m \end{bmatrix}$$

Jacobian matrix for F and V are

$$J_F = \begin{bmatrix} \beta_1 S_h & \beta_2 S_h \\ \mu S_m & 0 \end{bmatrix} \text{and } J_V = \begin{bmatrix} k_1 & 0 \\ 0 & k_2 \end{bmatrix}$$

at equilibrium point $E_0 = (\frac{\Lambda_h}{k_1}, 0, \frac{\Lambda_m}{k_2}, 0)$

$$J_F(E_0) = \begin{bmatrix} \frac{\beta_1 \Lambda_h}{k_1} & \frac{\beta_2 \Lambda_h}{k_1} \\ \frac{\mu \Lambda_m}{k_2} & 0 \end{bmatrix} \text{and } J_V(E_0) = \begin{bmatrix} k_1 & 0 \\ 0 & k_2 \end{bmatrix}$$

The reproduction number is obtain from eigen value of $J_F J_V^{-1}$
consider,

$$J_F(E_0)J_V^{-1}(E_0) = \begin{bmatrix} \frac{\beta_1\Lambda_h}{k_1} & \frac{\beta_2\Lambda_h}{k_1} \\ \frac{\mu\Lambda_m}{k_2} & 0 \end{bmatrix} \cdot \begin{bmatrix} \frac{1}{k_1} & 0 \\ 0 & \frac{1}{k_2} \end{bmatrix}$$

$$= \begin{bmatrix} \frac{\beta_1\Lambda_h}{k_1^2} & \frac{\beta_2\Lambda_h}{k_1k_2} \\ \frac{\mu\Lambda m}{k_1k_2} & 0 \end{bmatrix}$$

The basic reproduction number is the eigen value of above matrix and given by

$$R_0 = \frac{\beta_1\Lambda_h k_2 + \sqrt{\beta_1^2\Lambda_h^2k_2^2 + 4k_1^2\beta_2\mu\Lambda_h\Lambda_m}}{2k_1^2k_2}$$

1.4. **Stability Analysis.** The stability analysis of the mathematical model involves determining whether the disease-free equilibrium point is stable. This equilibrium occurs when there are no infected individuals in the population. Stability analysis typically involves examining the eigenvalues of the Jacobian matrix evaluated at the disease-free equilibrium point. If all eigenvalues have negative real parts, the equilibrium is stable. Conversely, if any eigenvalue has a positive real part, the equilibrium is unstable.
Consider the Jacobian Matrix of system 2,

$$J = \begin{bmatrix} -k_1 & -\beta_1 S_{h_0} & 0 & -\beta_2 S_{h_0} \\ \beta_1 I_{h_0} + \beta_2 I_{m_0} & \beta_1 S_{h_0} - k_1 & 0 & \beta_2 S_{h_0} \\ 0 & -\mu S_{m_0} & -k_2 & 0 \\ 0 & \mu S_{m_0} & 0 & -k_2 \end{bmatrix}$$

At equilibrium point $E_0 = (\frac{\Lambda_h}{k_1}, 0, \frac{\Lambda_m}{k_2}, 0)$,

$$J(E_0) = \begin{bmatrix} -k_1 & -\beta_1\frac{\Lambda_h}{k_1} & 0 & -\beta_2\frac{\Lambda_h}{k_1} \\ 0 & \beta_1\frac{\Lambda_h}{k_1} - k_1 & 0 & \beta_2\frac{\Lambda_h}{k_1} \\ 0 & -\mu\frac{\Lambda_m}{k_2} & -k_2 & 0 \\ 0 & \mu\frac{\Lambda_m}{k_2} & 0 & -k_2 \end{bmatrix}$$

The Characteristic equation of $J(E_0) - \lambda I$ is obtained as

$$\begin{bmatrix} -k_1 - \lambda & -\beta_1\frac{\Lambda_h}{k_1} & 0 & -\beta_2\frac{\Lambda_h}{k_1} \\ 0 & \beta_1\frac{\Lambda_h}{k_1} - k_1 - \lambda & 0 & \beta_2\frac{\Lambda_h}{k_1} \\ 0 & -\mu\frac{\Lambda_m}{k_2} & -k_2 - \lambda & 0 \\ 0 & \mu\frac{\Lambda_m}{k_2} & 0 & -k_2 - \lambda \end{bmatrix} = 0$$

$$\begin{bmatrix} A & B \\ C & D \end{bmatrix} = 0$$

Where,

$$A = \begin{bmatrix} -k_1 - \lambda & -\beta_1\frac{\Lambda_h}{k_1} \\ 0 & \beta_1\frac{\Lambda_h}{k_1} - k_1 - \lambda \end{bmatrix}$$

$$B = \begin{bmatrix} 0 & -\beta_2\frac{\Lambda_h}{k_1} \\ 0 & \beta_2\frac{\Lambda_h}{k_1} \end{bmatrix}$$

$$C = \begin{bmatrix} 0 & -\mu\frac{\Lambda_m}{k_2} \\ 0 & \mu\frac{\Lambda_m}{k_2} \end{bmatrix}$$

$$D = \begin{bmatrix} -k_2-\lambda & 0 \\ 0 & -k_2-\lambda \end{bmatrix}$$

The eigen values of $J(E_0)$ is same as the eigen values of $A\&D$.
The eigen values of A can be obtained by

$$\begin{bmatrix} -k_1-\lambda & -\beta_1\frac{\Lambda_h}{k_1} \\ 0 & \beta_1\frac{\Lambda_h}{k_1}-k_1-\lambda \end{bmatrix} = 0$$

$$(-k_1-\lambda)(\beta_1\frac{\Lambda_h}{k_1}-k_1-\lambda) = 0$$

$$-k_1\frac{\beta_1\Lambda_h}{k_1}+k_1^2+k_1\lambda-\lambda\frac{\beta_1\Lambda_h}{k_1}+k_1\lambda+\lambda^2 = 0$$

$$\lambda^2+\lambda(2k_1-\frac{\beta_1\Lambda_h}{k_1})+k_1^2-\beta_1\Lambda_h = 0$$

$$\lambda = \frac{-(2k_1-\frac{\beta_1\Lambda_h}{k_1}) \pm \sqrt{4k_1^2-\frac{4k_1\beta_1\Lambda h}{k_1}+\frac{\beta_1^2\Lambda_h^2}{k_1^2}-4k_1^2+4\beta_1\Lambda_h}}{2}$$

$$\lambda = \frac{-2k_1+\frac{\beta_1\Lambda_h}{k_1} \pm \frac{\beta_1\Lambda_h}{k_1}}{2}$$

$$\lambda = \frac{-2k_1+\frac{\beta_1\Lambda_h}{k_1} - \frac{\beta_1\Lambda_h}{k_1}}{2} \quad or \quad \frac{-2k_1+\frac{\beta_1\Lambda_h}{k_1} + \frac{\beta_1\Lambda_h}{k_1}}{2}$$

$$\lambda = -k_1 \quad or \quad -(k_1+\frac{\beta_1\Lambda_h}{k_1})$$

$$\therefore \lambda = -k_1 \quad or \quad -(k_1+\frac{\beta_1\Lambda_h}{k_1})$$

The eigen values of D can be obtained by

$$D = \begin{bmatrix} -k_2-\lambda & 0 \\ 0 & -k_2-\lambda \end{bmatrix}$$

$$(k_2+\lambda)^2 - 0 = 0$$

$$\lambda = -k_2 \ , \ -k_2$$

Since all the parameters are positive, $\lambda < 0$ for all the cases.
The model is stable as all the eigen values are negative.

2. Preliminary definition

We suggest modifications to certain fundamental definitions and preliminary concepts utilized in this study concerning fractional derivatives and integrals, which possess numerous properties and definitions.

Definition 2.1. *The Riemann-Liouville integral of a function $\mathcal{F}(t) \in \mathbf{C}_\delta$ ($\delta \geq -1$) having fractional order ($\eta > 0$) is presented as follows [12–15]:*

$$\mathcal{J}^\eta\mathcal{F}(t) = \frac{1}{\Gamma(\zeta)}\int_0^t (tv)^{\zeta-1}\mathcal{F}(v)dv, \tag{6}$$

$$\mathcal{J}^0\mathcal{F}(t) = \mathcal{F}(t). \tag{7}$$

Definition 2.2. *The Caputo fractional derivative of $\mathcal{F} \in \mathbf{C}^m_{-1}$ is presented as follows [12, 15]:*

$$\mathcal{D}^\delta_t\mathcal{F}(t) = \frac{1}{\Gamma(m-\delta)}\int_0^t (t-v)^{m-\delta-1}\mathcal{F}(v)dv, m-1 < \delta \leq m, m \in \mathbb{N}. \tag{8}$$

Definition 2.3. *The Natural Transform (NT) of $\mathcal{F}(t)$ is denoted by $\mathcal{N}[\mathcal{F}(t)]$ for $t \in \mathbb{R}$ and defined as [15, 17]*

$$\mathcal{N}[\mathcal{F}(t)] = \mathcal{R}[s,\omega] = \int_{-\infty}^{\infty} e^{-st}\mathcal{F}(\omega t)dt,\ \ s,\omega \in (-\infty,\infty), \tag{9}$$

where s and ω are the NT variables. Now, we present NT as

$$\mathcal{N}[\mathcal{F}(t)\mathcal{H}(t)] = \mathcal{N}^+[\mathcal{F}(t)] = \mathcal{R}^+(s,\omega) = \int_0^{\infty} e^{-st}\mathcal{F}(\omega t)dt,\ \ s,\omega \in (0,\infty), and\ t \in \mathbb{R}, \tag{10}$$

where $\mathcal{H}(t)$ symbolises the Heaviside function. Further, for $s = 1$, the Eq. (10) signifies the Sumudu transform and for $\omega = 1$, Eq. (10) is simplifies to the Laplace transform.

Definition 2.4. *For the function $\mathcal{R}(s,\omega)$, the inverse NT is stated as [15]*

$$\mathcal{N}^{-1}[\mathcal{R}(s,\omega)] = \mathcal{F}(t), \forall\ t \geq 0. \tag{11}$$

Theorem 2.1. *If $\mathcal{R}(s,\omega)$ is the natural transform of $\mathcal{F}(t)$, then the natural transform of the Riemann-Liouville fractional integral for $\mathcal{F}(t)$ of order δ denoted by $\mathcal{J}^\delta\mathcal{F}(t)$ is given by*

$$\mathcal{N}^+[\mathcal{J}^\delta\mathcal{F}(t)] = \frac{\omega^\delta}{s^\delta}\mathcal{R}(s,\omega). \tag{12}$$

Theorem 2.2. *Let $\mathcal{R}(s,\omega)$ be the natural transform of $\mathcal{F}(t)$, then the NT $\mathcal{R}_\delta(s,\omega)$ of the Riemann-Liouville fractional derivative of $\mathcal{F}(t)$ is denoted by $\mathcal{D}^\delta\mathcal{F}(t)$ and defined as*

$$\mathcal{N}^+[\mathcal{D}^\delta\mathcal{F}(t)] = \mathcal{R}_\delta(s,\omega) = \frac{s^\delta}{\omega^\delta}\mathcal{R}(s,\omega) - \sum_{k=0}^{m-1}\frac{s^k}{\omega^{\delta-k}}\left[\mathcal{D}^{\delta-k-1}\mathcal{F}(t)\right]_{t=0}, \tag{13}$$

where m be any positive integer and δ is the order. Further $m-1 \leq \delta < m$.

Theorem 2.3. *Let $\mathcal{R}(s,\omega)$ be the natural transform of $\mathcal{F}(t)$, then the NT $\mathcal{R}_\delta(s,\omega)$ of the Caputo fractional derivative of $\mathcal{F}(t)$ is denoted by ${}^c\mathcal{D}^\delta\mathcal{F}(t)$ and defined as*

$$\mathcal{N}^+[{}^c\mathcal{D}^\delta\mathcal{F}(t)] = \mathcal{R}^c_\delta(s,\omega) = \frac{s^\delta}{\omega^\delta}\mathcal{R}(s,\omega) - \sum_{k=0}^{m-1}\frac{s^{\delta-(k+1)}}{\omega^{\delta-k}}\left[\mathcal{D}^k\mathcal{F}(t)\right]_{t=0}, \tag{14}$$

where m is any positive integer and δ is the order. Further, $m-1 \leq \delta < m$.

2.1. Elementary Properties of NT.

(1) $\mathcal{N}^+[1] = \frac{1}{s}$,

(2) $\mathcal{N}^+[t^\delta] = \frac{\Gamma(\delta+1)\omega^\delta}{s^{\delta+1}}$,

(3) $\mathcal{N}^+[\mathcal{F}^m(t)] = \frac{s^m}{\omega^m}\mathcal{R}(s,\omega) - \sum_{k=0}^{m-1}\frac{s^{m-(k+1)}}{\omega^{m-k}}\frac{\Gamma(\delta+1)\omega^\delta}{s^{\delta+1}}$.

(4) (Convolution Theorem of NT) $\mathcal{N}^+[\mathcal{F}_1(t) * \mathcal{F}_2(t)] = \omega\mathcal{R}(s,\omega)\mathcal{G}(s,\omega)$.
(5) (NT-ST Duality (NSD)): If $\mathcal{R}(s,\omega)$ and $\mathcal{G}(\omega)$ are the Natural and Sumudu transform of $\mathcal{F}(t) \in A$, respectively, then

$$\mathcal{N}^+[\mathcal{F}(t)] = \mathcal{R}(s,\omega) = \frac{1}{s}\int_0^\infty e^{-t}\mathcal{F}\left(\frac{\omega t}{s}\right)\mathrm{d}t = \frac{1}{s}\mathcal{G}\left(\frac{\omega}{s}\right).$$

2.2. **The Fundamental Aspect of Natural Decomposition Transform.** To demonstrate the fundamental theory and solution procedure of FNDM, we consider

$$\mathcal{D}_t^\delta\omega(x,t) + \mathcal{R}\omega(x,t) + \mathcal{F}\omega(x,t) = h(x,t), \tag{15}$$

with initial condition

$$\omega(x,0) = g(x), \tag{16}$$

where $\mathcal{D}^\delta u(x,t)$ signifies the fractional Caputo derivative of $\omega(x,t), \mathcal{R}$ and $\mathcal{F}$ respectively are the linear and nonlinear differential operator, and $h(x,t)$ is the source term. On applying NT and by the assist of Theorem 2, then(15) provides

$$\mathcal{U}(x,s,\omega) = \frac{\omega^\delta}{s^\delta}\sum_{k=0}^{n-1}\frac{s^{\delta-(k+1)}}{\omega^{\delta-k}}[\mathcal{D}^k\omega(x,t)]_{t=0} + \frac{\omega^\delta}{s^\delta}\mathcal{N}^+[h(x,t)] - \frac{\omega^\delta}{s^\delta}\mathcal{N}^+[\mathcal{R}\omega(x,t) + \mathcal{F}\omega(x,t)] \tag{17}$$

Apply the inverse NT on Eq(17) to get

$$\omega(x,t) = \mathcal{G}(x,t) - \mathcal{N}^{-1}\left[\frac{\omega^\delta}{S^\delta}\mathcal{N}^+[\mathcal{R}\omega(x,t) + \mathcal{F}\omega(x,t)]\right] \tag{18}$$

From non-homogeneous term and given initial condition, $\mathcal{G}(x,t)$ is exists. The infinite series solution is defined as follows

$$\omega(x,t) = \sum_{n=0}^\infty \omega_n(x,t), \quad \mathcal{F}\omega(x,t) = \sum_{n=0}^\infty \mathcal{A}_n, \tag{19}$$

Where the $\mathcal{A}_n$ is indicating the nonlinear term of $\mathcal{F}\omega(x,t)$. By using the Eqs(18) and (19), we have

$$\sum_{n=0}^\infty \omega_n(x,t) = \mathcal{G}(x,t) - \mathcal{N}^{-1}\left[\frac{\omega^\delta}{S^\delta}\mathcal{N}^+\left[\mathcal{R}\sum_{n=0}^\infty \omega_n(x,t)\right] + \sum_{n=0}^\infty \mathcal{A}_n\right] \tag{20}$$

By comparing both sides of Eq(20), we obtain

$$\omega_0(x,t) = G(x,t),$$
$$\omega_1(x,t) = -N^{-1}\left[\frac{\omega^\delta}{s^\delta}\mathcal{N}^+[\mathcal{R}\omega_0(x,t)] + \mathcal{A}_0\right],$$
$$u\omega_2(x,t) = -N^{-1}\left[\frac{\omega^\delta}{s^\delta}\mathcal{N}^+[\mathcal{R}\omega_1(x,t)] + \mathcal{A}_1\right],$$
$$\vdots$$

Similarly, we obtain the recursive relation in general form for $n \geq 1$ and define as

$$\omega_{n+1}(x,t) = -N^{-1}\left[\frac{\omega^\delta}{s^\delta}\mathcal{N}^+[\mathcal{R}\omega_n(x,t)] + \mathcal{A}_n\right], \tag{21}$$

Lastly, the approximate solution is defined as follows

$$\omega(x,t) = \sum_{n=0}^{\infty} \omega_n(x,t). \tag{22}$$

2.3. **Convergence Analysis & Uniqueness of FNDM Solution.** In this section, we explore the uniqueness and convergence of the FNDM to gain a better understanding of its properties.

Theorem 2.4. *[15] Let $|R(\omega) - R(\omega^*)| < \lambda_1|\omega - \omega^*|$ and $|F(\omega) - F(\omega^*)| < \lambda_2|\omega - \omega^*|$, where $m\colon = \omega(\beta,t)$ and $\omega^*\colon = \omega^*(\beta,t)$ are values of two different functions and λ_1, λ_2 are Lipschitz constants.*
R and F are the operators mentioned in (15). Then for FNDM the solution of (15) is unique when $0 < (\lambda_1 + \lambda_2)(1 - \beta + \beta t) < 1$ for all t.

Theorem 2.5. *Let $I : \mathcal{H} \to \mathcal{H}$ be a nonlinear operator and let m be an exact solution of (15). $\sum_{i=0}^{\infty} \omega_i$, which is obtained by (22), converges to ω, if $\exists\ \lambda, 0 \le \lambda < 1$, such that $\|\omega_{k+1}\| \le \lambda\|\omega_k\|, \forall\ k \in \mathbb{N} \cup \{0\}$.*

3. Approximate Solutions of Fractional Zika virus Model

Applying the NT and Theorem (2.3) to both sides of Eq. (2), we obtain

$$\begin{aligned}
S_h(s,\omega) &= \frac{1}{s}S_h(0) + \frac{\omega^\delta}{s^\delta}\mathcal{N}^+\left[\Lambda_h - \beta_1 S_h I_h - \beta_2 S_h I_m - k_1 S_h\right]\\
I_h(s,\omega) &= \frac{1}{s}I_h(0) + \frac{\omega^\delta}{s^\delta}\mathcal{N}^+\left[\beta_1 S_h I_h + \beta_2 S_h I_m - k_1 I_h\right]\\
S_m(s,\omega) &= \frac{1}{s}S_m(0) + \frac{\omega^\delta}{s^\delta}\mathcal{N}^+\left[\Lambda_m - \mu S_m I_h - k_2 S_m\right]\\
I_m(s,\omega) &= \frac{1}{s}I_m(0) + \frac{\omega^\delta}{s^\delta}\mathcal{N}^+\left[\mu S_m I_h - k_2 I_m\right]
\end{aligned} \tag{23}$$

Using the initial conditions into a system of Eq. (23), we obtain

$$\begin{aligned}
S_h(s,\omega) &= \frac{1}{s}800 + \frac{\omega^\delta}{s^\delta}\mathcal{N}^+\left[(1.2) - (0.125\times10^{-4})S_h I_h - (0.4\times10^{-4})S_h I_m - (0.004)S_h\right]\\
I_h(s,\omega) &= \frac{1}{s}200 + \frac{\omega^\delta}{s^\delta}\mathcal{N}^+\left[(0.125\times10^{-4})S_h I_h + (0.4\times10^{-4})S_h I_m - (0.004)I_h\right]\\
S_m(s,\omega) &= \frac{1}{s}600 + \frac{\omega^\delta}{s^\delta}\mathcal{N}^+\left[(0.3) - (0.475\times10^{-5})S_m I_h - (0.0014)S_m\right]\\
I_m(s,\omega) &= \frac{1}{s}300 + \frac{\omega^\delta}{s^\delta}\mathcal{N}^+\left[(0.475\times10^{-5})S_m I_h - (0.0014)I_m\right]
\end{aligned} \tag{24}$$

Apply the inverse NT to Eq. (24) to obtain

$$
\begin{aligned}
S_h(t) &= 800 \\
&\quad + \mathcal{N}^{-1}\left[\frac{\omega^\delta}{s^\delta}\mathcal{N}^+\left[(1.2) - (0.125\times 10^{-4})S_hI_h - (0.4\times 10^{-4})S_hI_m - (0.004)S_h\right]\right] \\
I_h(t) &= 200 + \mathcal{N}^{-1}\left[\frac{\omega^\delta}{s^\delta}\mathcal{N}^+\left[(0.125\times 10^{-4})S_hI_h + (0.4\times 10^{-4})S_hI_m - (0.004)I_h\right]\right] \\
S_m(t) &= 600 + \mathcal{N}^{-1}\left[\frac{\omega^\delta}{s^\delta}\mathcal{N}^+\left[(0.3) - (0.475\times 10^{-5})S_mI_h - (0.0014)S_m\right]\right] \\
I_m(t) &= 300 + \mathcal{N}^{-1}\left[\frac{\omega^\delta}{s^\delta}\mathcal{N}^+\left[(0.475\times 10^{-5})S_mI_h - (0.0014)I_m\right]\right]
\end{aligned} \tag{25}
$$

Assume an infinite series solution for the unknown functions $S_h(t), I_h(t), S_m(t)$, and $I_m(t)$ of the form

$$
S_h(t) = \sum_{n=0}^{\infty} S_{h_n}(t), I_h(t) = \sum_{n=0}^{\infty} I_{h_n}(t), S_m(t) = \sum_{n=0}^{\infty} S_{m_n}(t), I_m(t) = \sum_{n=0}^{\infty} I_{m_n}(t) \tag{26}
$$

Using Eq. (26), we can rewrite Eq. (24) in the form

$$
\begin{aligned}
\sum_{n=0}^{\infty} S_{h_n}(t) &= 800 + \mathcal{N}^{-1}\Big[\frac{\omega^\delta}{s^\delta}\mathcal{N}^+ \\
&\quad \left[(1.2) - (0.125\times 10^{-4})\sum_{n=0}^{\infty}\mathcal{A}_n - (0.4\times 10^{-4})\sum_{n=0}^{\infty}\mathcal{B}_n - (0.004)\sum_{n=0}^{\infty} S_{h_n}(t)\right]\Big] \\
\sum_{n=0}^{\infty} I_{h_n}(t) &= 200 + \mathcal{N}^{-1}\Big[\frac{\omega^\delta}{s^\delta}\mathcal{N}^+ \\
&\quad \left[(0.125\times 10^{-4})\sum_{n=0}^{\infty}\mathcal{A}_n + (0.4\times 10^{-4})\sum_{n=0}^{\infty}\mathcal{B}_n - (0.004)\sum_{n=0}^{\infty} I_{h_n}(t)\right]\Big] \\
\sum_{n=0}^{\infty} S_{m_n}(t) &= 600 \\
&\quad + \mathcal{N}^{-1}\left[\frac{\omega^\delta}{s^\delta}\mathcal{N}^+\left[(0.3) - (0.475\times 10^{-5})\sum_{n=0}^{\infty}\mathcal{C}_n - (0.0014)\sum_{n=0}^{\infty} S_{m_n}(t)\right]\right] \\
\sum_{n=0}^{\infty} I_{m_n}(t) &= 300 + \mathcal{N}^{-1}\left[\frac{\omega^\delta}{s^\delta}\mathcal{N}^+\left[(0.475\times 10^{-5})\sum_{n=0}^{\infty}\mathcal{C}_n - (0.0014)\sum_{n=0}^{\infty} I_{m_n}(t)\right]\right]
\end{aligned} \tag{27}
$$

where, $\mathcal{A}_n, \mathcal{B}_n$, and $\mathcal{C}_n$ are the Adomian polynomials that represents the nonlinear term $S_{hn}(t)I_{hn}(t), S_{hn}(t)I_{mn}(t)$, and $S_{mn}(t)I_{hn}(t)$ resp. Then by comparing both sides of Eq. (27), we can easily generate the recursive relation as follows:

$$
\begin{aligned}
S_{h_0}(t) &= 800 \\
I_{h_0}(t) &= 200 \\
S_{m_0}(t) &= 600 \\
I_{m_0}(t) &= 300
\end{aligned}
$$

$$S_{h_1}(t) = \mathcal{N}^{-1}\left[\frac{\omega^\delta}{s^\delta}\mathcal{N}^+\left[(1.2) - (0.125\times 10^{-4})\mathcal{A}_0 - (0.4\times 10^{-4})\mathcal{B}_0 - (0.004)S_{h_0}(t)\right]\right]$$
$$I_{h_1}(t) = \mathcal{N}^{-1}\left[\frac{\omega^\delta}{s^\delta}\mathcal{N}^+\left[(0.125\times 10^{-4})\mathcal{A}_0 + (0.4\times 10^{-4})\mathcal{B}_0 - (0.004)I_{h_0}(t)\right]\right]$$
$$S_{m_1}(t) = \mathcal{N}^{-1}\left[\frac{\omega^\delta}{s^\delta}\mathcal{N}^+\left[(0.3) - (0.475\times 10^{-5})\mathcal{C}_0 - (0.0014)S_{m_0}(t)\right]\right]$$
$$I_{m_1}(t) = \mathcal{N}^{-1}\left[\frac{\omega^\delta}{s^\delta}\mathcal{N}^+\left[(0.475\times 10^{-5})\mathcal{C}_0 - (0.0014)I_{m_0}(t)\right]\right]$$

$$S_{h_2}(t) = \mathcal{N}^{-1}\left[\frac{\omega^\delta}{s^\delta}\mathcal{N}^+\left[(1.2) - (0.125\times 10^{-4})\mathcal{A}_1 - (0.4\times 10^{-4})\mathcal{B}_1 - (0.004)S_{h_1}(t)\right]\right]$$
$$I_{h_2}(t) = \mathcal{N}^{-1}\left[\frac{\omega^\delta}{s^\delta}\mathcal{N}^+\left[(0.125\times 10^{-4})\mathcal{A}_1 + (0.4\times 10^{-4})\mathcal{B}_1 - (0.004)I_{h_1}(t)\right]\right]$$
$$S_{m_2}(t) = \mathcal{N}^{-1}\left[\frac{\omega^\delta}{s^\delta}\mathcal{N}^+\left[(0.3) - (0.475\times 10^{-5})\mathcal{C}_1 - (0.0014)S_{m_1}(t)\right]\right]$$
$$I_{m_2}(t) = \mathcal{N}^{-1}\left[\frac{\omega^\delta}{s^\delta}\mathcal{N}^+\left[(0.475\times 10^{-5})\mathcal{C}_1 - (0.0014)I_{m_1}(t)\right]\right]$$

We continue in this manner to obtain

$$S_{h_{n+1}}(t) = \mathcal{N}^{-1}\left[\frac{\omega^\delta}{s^\delta}\mathcal{N}^+\left[(1.2) - (0.125\times 10^{-4})\mathcal{A}_n - (0.4\times 10^{-4})\mathcal{B}_n - (0.004)S_{h_n}(t)\right]\right]$$
$$I_{h_{n+1}}(t) = \mathcal{N}^{-1}\left[\frac{\omega^\delta}{s^\delta}\mathcal{N}^+\left[(0.125\times 10^{-4})\mathcal{A}_n + (0.4\times 10^{-4})\mathcal{B}_n - (0.004)I_{h_n}(t)\right]\right]$$
$$S_{m_{n+1}}(t) = \mathcal{N}^{-1}\left[\frac{\omega^\delta}{s^\delta}\mathcal{N}^+\left[(0.3) - (0.475\times 10^{-5})\mathcal{C}_n - (0.0014)S_{m_n}(t)\right]\right]$$
$$I_{m_{n+1}}(t) = \mathcal{N}^{-1}\left[\frac{\omega^\delta}{s^\delta}\mathcal{N}^+\left[(0.475\times 10^{-5})\mathcal{C}_n - (0.0014)I_{m_n}(t)\right]\right] \tag{28}$$

Using Eq. (28), we can easily compute the remaining components as follows:

$$S_{h_1}(t) = -13.6\ \frac{t^\delta}{\Gamma(\delta+1)}$$
$$I_{h_1}(t) = 10.8\ \frac{t^\delta}{\Gamma(\delta+1)}$$
$$S_{m_1}(t) = -1.11\ \frac{t^\delta}{\Gamma(\delta+1)}$$
$$I_{m_1}(t) = 0.15\ \frac{t^\delta}{\Gamma(\delta+1)}$$

$$S_{h_2}(t) = 1.2\ \frac{t^{\delta}}{\Gamma(\delta+1)} + \frac{0.1388\ t^{2\delta}}{\Gamma(2\delta+1)}$$
$$I_{h_2}(t) = -\frac{0.1276\ t^{2\delta}}{\Gamma(2\delta+1)}$$
$$S_{m_2}(t) = 0.3\ \frac{t^{\delta}}{\Gamma(\delta+1)} - \frac{0.0281715\ t^{2\delta}}{\Gamma(2\delta+1)}$$
$$I_{m_2}(t) = \frac{0.0295155\ t^{2\delta}}{\Gamma(2\delta+1)}.$$

We continue in this manner, and after two iterations, we obtain the approximate solution given by

$$\begin{aligned} S_h(t) &= \sum_{n=0}^{\infty} S_{h_n}(t) \\ &= 800 - 13.6\ \frac{t^{\delta}}{\Gamma(\delta+1)} + 1.2\ \frac{t^{\delta}}{\Gamma(\delta+1)} + \frac{0.1388\ t^{2\delta}}{\Gamma(2\delta+1)} \end{aligned} \tag{29}$$

$$\begin{aligned} I_h(t) &= \sum_{n=0}^{\infty} I_{h_n}(t) \\ &= 200 + 10.8\ \frac{t^{\delta}}{\Gamma(\delta+1)} - \frac{0.1276\ t^{2\delta}}{\Gamma(2\delta+1)} + \cdots \end{aligned} \tag{30}$$

$$\begin{aligned} S_m(t) &= \sum_{n=0}^{\infty} S_{m_n}(t) \\ &= 600 - 1.11\ \frac{t^{\delta}}{\Gamma(\delta+1)} + 0.3\ \frac{t^{\delta}}{\Gamma(\delta+1)} - \frac{0.0281715\ t^{2\delta}}{\Gamma(2\delta+1)} + \cdots \end{aligned} \tag{31}$$

$$\begin{aligned} I_m(t) &= \sum_{n=0}^{\infty} I_{m_n}(t) \\ &= 300 + 0.15\ \frac{t^{\delta}}{\Gamma(\delta+1)} + \frac{0.0295155\ t^{2\delta}}{\Gamma(2\delta+1)} + \cdots \end{aligned} \tag{32}$$

4. Discussion and Outcomes

In this section, we delve into the behavior of the solutions derived from the transmission model of the Zika virus as per system (2), utilizing numerical findings. The parameters of the model are set as follows: $\Lambda_h = 1.2, \Lambda_m = 0.3, k_1 = 0.004, k_2 = 0.0014, \beta_1 = 0.125 \times 10^{-4}, \beta_2 = 0.4 \times 10^{-4}$, and $\mu = 0.475 \times 10^{-5}$. Additionally, the initial values are designated as $S_h(0) = 800, I_h(0) = 200, S_m(0) = 600$, and $I_m(0) = 300$.

Fig. 2 illustrates the population of susceptible individuals (S_h), while Fig. 3 displays the population of infected individuals (I_h), considering both integer-order derivative ($\delta = 1$) and fractional-order derivatives ($\delta = 0.98, 0.96, 0.94, 0.92, 0.9$). In Fig. 2, it is evident that the trend of S_h remains consistent for both types of derivatives, gradually decreasing over time, indicating the increasing exposure of all healthy individuals to the disease. However, the numerical values obtained differ, with lower derivative orders yielding higher numerical outcomes.

Similarly, in Fig. 3, the behavior of I_h remains consistent across both derivatives, with varying numerical values. As the derivative order decreases, the numerical value for I_h increases noticeably over time, with a significant discrepancy in values observed. Notably,

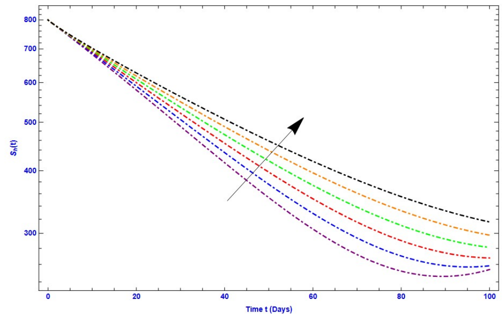

FIGURE 2. Plots illustrating the susceptible population, $S_h(t)$, are presented for both integer-order derivative at $\delta = 1$ and fractional-order derivatives with δ values ranging from 0.98 to 0.90.

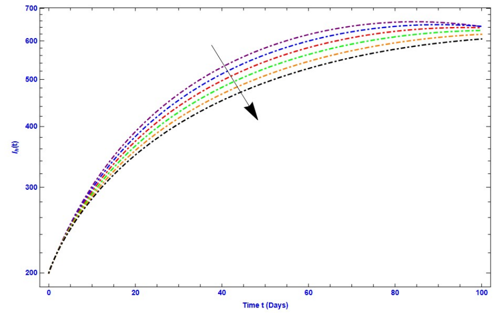

FIGURE 3. Plots illustrating the infected population, $I_h(t)$, are presented for both integer-order derivative at $\delta = 1$ and fractional-order derivatives with δ values ranging from 0.98 to 0.90.

Fig. 3 depicts I_h reaching its peak within the initial 100 days, followed by a gradual decline towards an equilibrium point.
Figs. 4 and 5 depict susceptible mosquitoes (S_m) and infected mosquitoes (I_m) respectively. The behavior of these functions remains consistent across both derivatives, with differing numerical outcomes. Over time, the population of healthy mosquitoes diminishes, indicating increased exposure to the disease, while the population of infected mosquitoes steadily rises.

5. CONCLUSION

We have developed a novel fractional-order mathematical model to analyze the transmission dynamics of the Zika virus. By incorporating a fractional-order Caputo derivative, we have established sufficient conditions for the existence, uniqueness, and stability of both disease-free in terms of the basic reproduction number. Furthermore, we have demonstrated the positivity and boundedness of solutions within a feasible region. To validate our theoretical findings, we have conducted numerical simulations using the Fractional Natural Decomposition Method for specific parameter settings: $\Lambda_h = 1.2, \Lambda_m = 0.3, k_1 = 0.004, k_2 = 0.0014, \beta_1 = 0.125 \times 10^{-4}, \beta_2 = 0.4 \times 10^{-4}$, and $\mu = 0.475 \times 10^{-5}$. Additionally, the initial values are designated as $S_h(0) = 800, I_h(0) = 200, S_m(0) = 600$, and $I_m(0) = 300.$, highlighting the influence of fractional derivatives on the dynamics of disease transmission.
Fractional calculus has gained significant attention in recent years due to its effectiveness in modeling complex real-world phenomena, including infectious disease dynamics. Researchers have successfully applied fractional-order models to study diseases such as HIV, AIDS, and COVID-19, capturing memory effects and nonlocal influences more accurately than classical models. In future work, we aim to explore the qualitative and numerical aspects of our proposed model under different fractional-order derivatives using real data. This ongoing research will provide deeper insights into the impact of fractional dynamics on Zika virus transmission and contribute to the development of more effective control strategies. Our findings will be reported in a future publication.

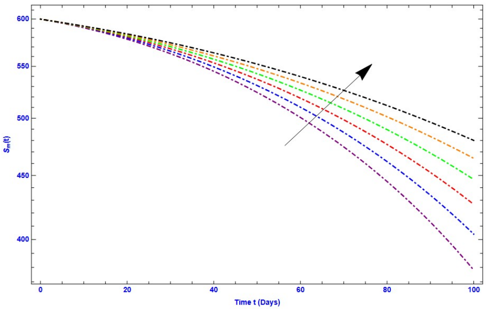

Figure 4. Graphs depicting the susceptible mosquito population, $S_m(t)$, are displayed for both the integer-order derivative at $\delta = 1$ and fractional-order derivatives with varying values of δ, including $0.98, 0.96, 0.94, 0.92,$ and 0.90.

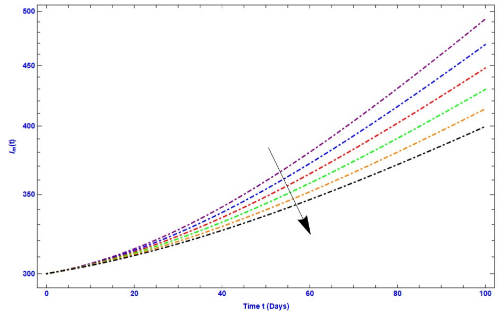

Figure 5. Graphs depicting the infected mosquito population, $I_m(t)$, are displayed for both the integer-order derivative at $\delta = 1$ and fractional-order derivatives with varying values of δ, including $0.98, 0.96, 0.94, 0.92,$ and 0.90.

Acknowledgement. The authors would like to extend their gratitude to Center of Education, Indian Institute of Teacher Education, Gandhinagar, Gujarat, India, for providing research facilities.

References

[1] Plourde, A. R. and Bloch, E. M., (2016), A literature review of Zika virus. Emerging infectious diseases, 22(7), p.1185.

[2] Song, B. H., Yun, S. I., Woolley, M. and Lee, Y.M., (2017), Zika virus: History, epidemiology, transmission, and clinical presentation. Journal of neuroimmunology, 308, pp.50-64.

[3] Sharma, A. and Lal, S. K., (2017), Zika virus: transmission, detection, control, and prevention. Frontiers in microbiology, 8, p.110.

[4] Manguin, S. and Boëte, C., (2011), Global impact of mosquito biodiversity, human vector-borne diseases and environmental change. The importance of biological interactions in the study of biodiversity, pp.27-50.

[5] Madzlan, F., Dom, N. C., Tiong, C. S. and Zakaria, N., (2016), Breeding characteristics of Aedes mosquitoes in dengue risk area. Procedia-Social and Behavioral Sciences, 234, pp.164-172.

[6] Musso, D. and Gubler, D. J., (2015), Zika virus: following the path of dengue and chikungunya?. The Lancet, 386(9990), pp.243-244.

[7] Yavuz, M. and Abdeljawad, T., (2020), Nonlinear regularized long-wave models with a new integral transformation applied to the fractional derivative with power and Mittag-Leffler kernel. Advances in Difference Equations, 2020(1), p.367.

[8] Shah, K., Alqudah, M. A., Jarad, F. and Abdeljawad, T., (2020), Semi-analytical study of Pine Wilt Disease model with convex rate under Caputo–Febrizio fractional order derivative. Chaos, Solitons & Fractals, 135, p.109754.

[9] Bekiryazici, Z., Kesemen, T., Merdan, M. and Khaniyev, T., (2023), Modeling Disease Transmission Dynamics with Random Data and Heavy Tailed Random Effects: The Zika Case. TWMS Journal of Applied & Engineering Mathematics, 13(4).

[10] Elsaka, H. and Ahmed, E., (2016), A fractional order network model for ZIKA. BioRxiv, p.039917.

[11] Rezapour, S., Mohammadi, H. and Jajarmi, A., (2020), A new mathematical model for Zika virus transmission. Advances in difference equations, 2020(1), pp.1-15.

[12] Zhou, M. X., Kanth, A. R., Aruna, K., Raghavendar, K., Rezazadeh, H., Inc, M. and Aly, A. A., (2021), Numerical Solutions of Time Fractional Zakharov-Kuznetsov Equation via Natural Transform Decomposition Method with Nonsingular Kernel Derivatives. Journal of Function Spaces, 2021(1), p.9884027.

[13] Alderremy, A. A., Aly, S., Fayyaz, R., Khan, A., Shah, R. and Wyal, N., (2022), The Analysis of Fractional-Order Nonlinear Systems of Third Order KdV and Burgers Equations via a Novel Transform. Complexity, 2022(1), p.4935809.

[14] Sunthrayuth, P., Alyousef, H. A., El-Tantawy, S. A., Khan, A. and Wyal, N., (2022), Solving Fractional-Order Diffusion Equations in a Plasma and Fluids via a Novel Transform. Journal of Function Spaces, 2022(1), p.1899130.

[15] Al-Sawalha, M. M., Ababneh, O. Y., Shah, R. and Nonlaopon, K., (2023), Numerical analysis of fractional-order Whitham-Broer-Kaup equations with non-singular kernel operators. AIMS Mathematics, 8(1), pp.2308-2336.

[16] Shah K., Abdeljavad T., Ahmad I., (2024), On Non-linear Fractional Order Coupled Pantograph Differential Equations under Nonlocal Boundary Conditions, TWMS J. Pure Appl. Math., V.15, N.1, pp.65-78. DOI:10.30546/2219-1259.15.1.2024.1786

[17] Veeresha, P., Prakasha, D. G. and Singh, J., (2020), Solution for fractional forced KdV equation using fractional natural decomposition method. Aims Math, 5(2), pp.798-810.

[18] Ullah, M. Z., Alzahrani, A. K. and Baleanu, D., (2019), An efficient numerical technique for a new fractional tuberculosis model with nonsingular derivative operator. Journal of Taibah University for Science, 13(1), pp.1147-1157.

[19] Gómez-Aguilar, J. F., Rosales-García, J. J., Bernal-Alvarado, J. J., Córdova-Fraga, T. and Guzmán-Cabrera, R., (2012), Fractional mechanical oscillators. Revista mexicana de física, 58(4), pp.348-352.

[20] Begum, R., Tunç, O., Khan, H., Gulzar, H. and Khan, A., (2021), A fractional order Zika virus model with Mittag–Leffler kernel. Chaos, Solitons & Fractals, 146, p.110898.

[21] Goswami, N. K., Srivastav, A. K., Ghosh, M. and Shanmukha, B., (2018), Mathematical modeling of zika virus disease with nonlinear incidence and optimal control. In Journal of Physics: Conference Series (Vol. 1000, p. 012114). IOP Publishing.

[22] Suparit, P., Wiratsudakul, A. and Modchang, C., (2018), A mathematical model for Zika virus transmission dynamics with a time-dependent mosquito biting rate. Theoretical Biology and Medical Modelling, 15, pp.1-11.

[23] González-Parra, G. and Benincasa, T., (2019), Mathematical modeling and numerical simulations of Zika in Colombia considering mutation. Mathematics and Computers in Simulation, 163, pp.1-18.

[24] Agusto, F. B., Bewick, S. and Fagan, W. F., (2017), Mathematical model of Zika virus with vertical transmission. Infectious Disease Modelling, 2(2), pp.244-267.

[25] Anderson, R. M., (1991), Discussion: the Kermack-McKendrick epidemic threshold theorem. Bulletin of mathematical biology, 53, pp.1-32.

[26] Rodrigues, H. S., (2016), Application of SIR epidemiological model: new trends. arXiv preprint arXiv:1611.02565.

[27] Biswas, S. K., Ghosh, U. and Sarkar, S., (2024), A mathematical model of Zika virus transmission with saturated incidence and optimal control: A case study of 2016 zika outbreak in Puerto Rico. International Journal of Modelling and Simulation, 44(3), pp.172-189.

[28] Farman, M., Akgül, A., Sultan, M., Riaz, S., Asif, H., Agarwal, P. and Hassani, M. K., (2024), Numerical study and dynamics analysis of diabetes mellitus with co-infection of COVID-19 virus by using fractal fractional operator. Scientific Reports, 14(1), p.16489.

[29] Sharma, N., Singh, R., ul Rehman, A. and Agarwal, P., (2024), Approximate solutions of epidemic model of Zika virus. In Fractional Differential Equations (pp. 177-189). Academic Press.

[30] Danbaba, U. A., Aloko, M. D. and Ayinde, A. M., (2024), Mathematical modeling of mosquito borne diseases with vertical transmissions as applied to Dengue. International Journal of Mathematical Sciences and Optimization: Theory and Applications, 10(3), pp.31-56.

[31] Belgacem, F. B. M. and Silambarasan, R., (2012), Theory of natural transform. Math. Engg. Sci. Aeros, 3, pp.99-124.

[32] Shah, K., Patel, H. C., Jain, S. and Agarwal, P., (2024), Application of modified homotopy analysis transform method to fractional modified Kawahara equation. In Recent Trends in Fractional Calculus and Its Applications (pp. 273-284). Academic Press.

[33] Khan, Z. H. and Khan, W. A., (2008), N-transform properties and applications. Nust J. Eng. Sci, 1(1), pp.127-133.

[34] Shah, K., Junaid, M. and Ali, N., (2015), Extraction of Laplace, Sumudu, Fourier and Mellin transform from the natural transform. J. Appl. Environ. Biol. Sci, 5(9), pp.108-115.

[35] Hassani, H., Avazzadeh, Z., Agarwal, P., Mehrabi, S., Ebadi, M. J., Dahaghin, M.cS. and Naraghirad, E., (2023), A study on fractional tumor-immune interaction model related to lung cancer via generalized Laguerre polynomials. BMC medical research methodology, 23(1), p.189.

[36] Lanlege, D. I., Fadugba, S. E., Ali, N., Ozioko, A. L., Alam, N., Ahmad, S., Jeeva, N. and Sayed-Ahmed, M. Z., (2025), Mathematical model of the social pathogen of HIV/AIDS stigma, Commun. Math. Biol. Neurosci., (2025), p. 6.

[37] Dharmalingam, K. M., Jeeva, N., Ali, N., Al-Hamido, R. K., Fadugba, S. E., Malesela, K., Tolasa, F. T., El-Bahkiry, H. S. and Qousini, M., (2024), Mathematical analysis of Zika virus transmission: exploring semi-analytical solutions and effective controls. Commun. Math. Biol. Neurosci., (2024), p.112.

[38] Jeeva, N., Dharmalingam, K. M., Ali, N., Sayed-Ahmed, M. Z., Radwan, R. M., El-Bahkiry, H. S., Fadugba, S. E., Oshinubi, K., Malesela, K., Adeniji, A. and Tolasa, F. T., (2024), Epidemiology simulation: numerical techniques for analyzing type 2 diabetes model and its prevention measures, Commun. Math. Biol. Neurosci., (2024), p. 117.

[39] Omede, B. I., Bolaji, B., Peter, O. J., Ibrahim, A. A. and Oguntolu, F. A., 2024. Mathematical analysis on the vertical and horizontal transmission dynamics of HIV and Zika virus co-infection. Franklin Open, 6, p.100064.

[40] J. Zhou, X. Wu, C. Chen, (2025), Investigating Various Intuitionistic Fuzzy Information Measures and Their Relationships, Appl. Comput. Math., Vol.24, No.4,, pp.579-607. DOI: 10.30546/1683-6154.24.4.2025.579.

Dr. Kunjankumar N. Shah worked as an Assistant Professor (Level 11) in the Centre of Education, Faculty of Mathematics at Indian Institute of Teacher Education (IITE), Gandhinagar, Gujarat, India. Dr. Shah received his Ph.D. in Applied Mathematics from S.V National Institute of Technology (SVNIT), Surat, India. Dr. Shah's research interests mainly include Fluid Flow Through Porous Media, Epidemiology, Integral Transform, Homotopy Perturbation Method, Modified Homotopy Analysis Method, and Partial Differential Equation.

Jayashree Parmar received her B.Sc. B.Ed. degree from Indian institute of Teacher Education, Gandhinagar, Gujarat, indian and currently pursuing M.Sc. M.Ed. from Indian Institute of Teacher Education, Gandhinagar, Gujarat, India with a keen interest in Mathematics. Ms. Jayshree research interest include mathematical modeling of real world application and Epidemiology.

Jaydev S. Patel is working as an assistant professor in mathematics at L. D. College of Engineering. He has more than 13 years of experience of teaching engineering mathematics. He completed M.Sc. in 2006 from Gujarat University and obtained M.Phil. degree in 2012. Area of interest are linear algebra, differential equations and mathematical modelling. He is pursuing Ph.D. from Gujarat Technological University, Ahmedabad.

Prof. Himanshu C. Patel is a Professor at Dr. S. & S. S. Ghandhy Government Engineering College, Surat, Gujarat, India. Dr. Patel has worked on numerical modelling of some problems related to lubrication. The study of the effect of surface roughness incorporated in my PhD work suggests to carry out the effect of roughness at the nano scale on the performance of various types of bearings (particularly, circular plates, circular step, annular plates etc.)